Standardized high-dimensional spectral cytometry protocol and panels for whole blood immune phenotyping in clinical and translational studies

Tom Dott, Slobodan Culina, Rene Chemali, Cedric Ait Mansour, Florian Dubois, Bernd Jagla, Jean Marc Doisne, Lars Rogge, François Huetz, Friederike Jönsson, et al.

Hasan Milena (Orcid ID: 0000-0002-0879-7099)

Standardized high-dimensional spectral cytometry protocol and panels for whole blood immune phenotyping in clinical and translational studies

Tom Dott[1,2*], Slobodan Culina[1*], Rene Chemali[1], Cedric Ait Mansour[3], Florian Dubois[1,2], Bernd Jagla[1,4], Jean Marc Doisne[5], Lars Rogge[6], François Huetz[7], Friederike Jönsson[7,8], Pierre-Henri Commere[1], James Di Santo[5], Benjamin Terrier[9], Lluis Quintana-Murci[10], Darragh Duffy[1,2], Milena Hasan[1+], Milieu Intérieur Consortium

[1] Cytometry and Biomarkers UTechS, Institut Pasteur, Université Paris Cité, Paris, France
[2] Translational Immunology Unit, Institut Pasteur, Université Paris Cité, Paris, France
[3] Sony Europe BV, Surrey, United Kingdom
[4] Bioinformatics and Biostatistics Hub, Institut Pasteur, Université Paris Cité, France
[5] Innate Immunity Unit, Institut Pasteur, Université Paris Cité, France
[6] Immunoregulation Unit, Institut Pasteur, Université Paris Cité, France
[7] Unit of Antibodies in Therapy and Pathology, INSERM UMR1222, Institut Pasteur, Université de Paris Cité, Paris, France.
[8] CNRS, Paris, France
[9] Service de Médecine Interne, Hôpital Cochin, Paris, France
[10] Human Evolutionary Genetics Unit, CNRS, Institut Pasteur, Université Paris Cité, UMR2000, 75015 Paris, France

[*] These authors contributed equally

[+] Correspondence to:
Milena Hasan, Institut Pasteur, Université Paris Cité, Paris, France
e-mail: milena.hasan@pasteur.fr

Abstract

Flow cytometry is the method of choice for immunophenotyping in the context of clinical, translational, and systems immunology studies. Among the latter, the *Milieu Intérieur* (MI) project aims at defining the boundaries of a healthy immune response to identify determinants of immune response variation. MI used immunophenotyping of a 1000 healthy donor cohort by flow cytometry as a principal outcome for immune variance at steady state. New generation spectral cytometers now enable high-dimensional immune cell characterization from small sample volumes. Therefore, for the MI 10-year follow up study, we have developed two high-dimensional spectral flow cytometry panels for deep characterization of innate and adaptive whole blood immune cells (35 and 34 fluorescent markers, respectively). We have standardized the protocol for sample handling, staining, acquisition, and data analysis. This approach enables the reproducible quantification of over 182 immune cell phenotypes at a single site. We have applied the protocol to discern minor differences between healthy and patient samples and validated its value for application in immunomonitoring studies. Our protocol is currently used for characterization of the impact of age and environmental factors on peripheral blood immune phenotypes of >400 donors from the initial MI cohort.

This article has been accepted for publication and undergone full peer review but has not been through the copyediting, typesetting, pagination and proofreading process which may lead to differences between this version and the Version of Record. Please cite this article as doi: 10.1002/cyto.a.24801

Keywords

High-dimensional cell phenotyping, spectral cytometry, immunomonitoring, whole blood, PBMCs, systems immunology

INTRODUCTION

The human immune system provides diverse defense mechanisms against infectious pathogens and tumors. To study the complexity of such responses, numerous systems immunology projects have been developed in the last decade to perform in-depth characterization of immune subpopulations in large cohorts of healthy subjects. These studies aim to identify hereditary and non-hereditary determinants of variation in immune responses (1) and provide resources for identifying biomarkers of disease. Some examples include the Human Immunology Project Consortium (HIPC)(2); the European Network for Translational Immunology Research and Education (ENTIRE)(3); the 10 000 Immunome project (4); the Functional Genomics Project (5); the SardiNIA project (6), and the Milieu Interieur Consortium (MI) (7).

The Milieu Intérieur was initiated in 2011 with the aim of establishing the boundaries of a healthy immune response and identifying determinants of immune variability (7). As part of the initial phenotyping of the 1000 healthy donor cohort we developed (8) and applied ten 8-parameter flow cytometry panels to whole blood using a MACSQuant cytometer (Miltenyi Biotec). This analysis allowed us to identify genetic and environmental factors shaping circulating immune cell populations (9). To compare individual versus population aging effects on immunity we recently initiated a 10-year recall study of the original cohort. For cellular phenotyping of this new cohort, we took advantage of recent developments in multi-parameter flow cytometry.

These developments include high-dimensional conventional cytometers (e.g. Symphony A5, BD), new-generation mass cytometers (CyTOF), and recently developed spectral flow cytometers (Aurora, Cytek and ID7000, Sony Biotechnology)(10,11). These advances have been accompanied by the development of new fluorescent dyes and metal-tagged antibodies, which together led to an unprecedented dimensionality in the analysis of cell phenotypes. Spectral flow cytometry offers certain advantages as it allows for 1) simultaneous use of fluorophores of closely emitting spectra, incompatible with conventional flow cytometry; 2) expansion of immunophenotyping panel complexity to 40 parameters and beyond; and 3) measurement of cellular autofluorescence as a separate parameter to avoid false-positive signals. In this study, we describe the development of two 37/36-parameter panels for spectral cytometry that allow standardized immunophenotyping of major immune cell populations in human peripheral blood. In comparison to conventional methods, our approach is less time-consuming and allows for an in-depth analysis from low sample volumes, identification of rare cell subsets and weakly expressed antigens. It is highly compatible for applications to large population-based clinical and translational studies.

RESULTS

Choice of cytometer and Panel design

We selected the ID7000™ Spectral Cell Analyzer (Sony Biotechnology) based on a variety of technical features. The instrument has a unique sensitivity in detecting dim signals and rare cell populations and has an integrated deep-well plate reader. In addition, active mixing and cooling of the sample during the acquisition ensure stable acquisition flow rate and preservation of tandem dyes. Our ID7000 is configured with 6 lasers (320 nm, 355 nm, 405 nm, 488 nm, 561 nm, and 637 nm) and 184 detectors. Thanks to its capacity to efficiently identify and separate the dyes with near peak emission signals, spectral cytometry allowed us to characterize all immune cell phenotypes identified in the original MI study (9), and to add several other cell populations such as hematopoietic stem cells (HSC) in just two spectral panels.

We designed two complementary 35 and 34 fluorescent marker cytometry panels to enable identification of major innate and adaptive immune cell populations in 200µl of fresh blood each. Cell proportions, counts, the level of their surface antigen expression and their activation state were measured. A dead cell marker was included in both panels to permit gating on live cells. During the establishment of the panels, 106 different antibodies from four suppliers (BD Bioscience, Sony Biotechnology, ThermoFisher Scientific, Miltenyi Biotec) were tested, of which 43 were excluded (Supplementary table 1). All antibodies were titrated (in 3-5 dilutions) to fit the experimental conditions described in the protocol. Our selection criteria for panel validation were (a) specificity of the signal; (b) signal resolution; (c) availability of the desired fluorochrome; (d) fluorochrome stability (tandem dyes); and (e) price and availability of a single lot of reagents for a cohort study. The specificity of signal was evaluated based on the staining index, i.e., the difference between the positive and the negative populations and the spread of the negative population. Due to the high dimensionality of the panels, we were obliged to include three custom-made antibodies in the innate panel, to match the available fluorescent channels. To minimize the variation of fluorescent signal intensity, only one batch of each antibody was used for staining throughout the whole study. The innate and adaptive panels developed and validated in the study are depicted in Supplementary table 2.

Operating procedures

Sample preparation and acquisition

The staining protocol was modified from the initial MI study for immunophenotyping of 200µl of fresh whole blood and the acquisition step was standardized, as detailed in the Material and Methods section. We have not observed an added value of blocking Fc receptors (Supplementary Figure 1) and thus have not included this step in our protocols. Since the ID7000 spectral cytometer does not count cells, counting beads (123count eBeads™ Counting Beads, Invitrogen) were used to obtain absolute cell numbers. To each well, 50µl of bead suspension was added prior to the manual mixing step ahead of acquisition.

Data analysis

Gating strategies

In spectral analysis, signals from all detected channels are used to create one spectral emission signal, regardless of the number of fluorochromes analyzed. The unmixed data is typically visualized as a series of images or spectra, each representing the contribution of a

single dye to the overall signal. Therefore, the first step of data analysis consists of an unmixing procedure based on spectral libraries that enables identification of each individual fluorophore from a complex spectral signal of multiplexed dyes. The ID7000 uses the WLSM (Weighted Least Squares Method) fluorescence unmixing algorithm to separate the individual spectral fingerprints. Unmixed data are then converted to an FCS-compatible format. The gating strategy for both panels was validated using ID7000 and FlowJo software (version 10.9). We created FlowJo data analysis templates to ensure standardized gating strategy for both panels. The same software was used for manual data analysis that allowed characterization of over 182 cellular subsets and cell activation states. The scheme of all immune cell subpopulations and their phenotypes that can be identified with the two panels is presented in Figure 1A.

Innate panel

For characterizing major innate immune cell populations, we first identified $CD45^+$ hematopoietic cells, and then excluded doublets using FCS-A/FSC-H and SSC-A/SSC-H (Figure 1B). Subsequently, T and B cells ($CD3^+$ and $CD19^+$) were excluded from the subset of live cells to focus on innate subsets. CD16 and CD66b markers allowed us to identify eosinophils and neutrophils. Eosinophils were gated within $CD66b^+CD16^{-/low}$ population as $CD123^+CDw125^+$ cells, and neutrophils were gated as $CD66b^+CD16^+$ cells. The activation status of 3 subsets of granulocytes (gating strategy for basophils is described below) was assessed by their expression of CD16, CD32, CD63, CXCR4, FcεRI, HLA-DR, CD62L and PD-L1 molecules.

The $CD16^-$ cell population was further distinguished as $CD7^+$ or $CD7^-$. $CD7^+$ population was subsequently identified as NK cells if $CD16^+CD56^+$ and divided into two distinguished subsets ($CD56^{dim}CD16^{bright}$, $CD56^{bright}CD16^{dim}$) that were additionally characterized by their activation/inhibition status through the expression of CD56, CD69 and CD8a molecules. To identify ILCs, the $CD16^-CD56^-$ population was analyzed for the expression of NKG2A and CD94, and the double negative population further for CD127 expression. ILCs were identified among $CD127^+$ cells as $CD161^{-/low}$ $CD25^+$ and subdivided, by expression of CD117 and CRTh2, into ILC2 ($CRTh2^+CD117^{-/low}$), $CD117^-CRTh2^-$ and $CD117^+CRTh2^-$. Further gating of the $CD7^-$ population identified monocytes as $CD14^{+/-}CD16^+$ that were additionally subdivided into classical ($CD14^+CD16^{-/low}$), non-classical ($CD14^{dim}CD16^+$), and intermediate ($CD14^{med/+}CD16^+$) monocytes. We also assessed the expression of HLA-DR, CD4 and PD-L1 molecules within these populations as markers of activation.

In the population of $CD14^-CD16^-$ cells, $HLA\text{-}DR^+CD14^-$ cells were selected to subsequently segregate pDCs ($CD123^+CD11c^-$) from cDCs ($CD11c^+CD123^-$). cDCs were additionally divided into $CD141^+$ cDCs and $CD1c^+$ cDCs as $CD141^+CD1c^-$ and $CD141^-CD1c^+$, respectively. The activation status of the three DC subsets was assessed by their expression of HLA-DR, CD4, CD8a, CXCR4 and the costimulatory molecules CD86 and PD-L1.

The $CD14^-$ $HLA\text{-}DR^-$ population resolved by CD45, and CD123 staining was used to identify basophils as $CD45^{lo}CD123^+$ cells that were further gated as $CD123^+Fc\varepsilon RI^+$ cells. Stem cells were identified as not $CD45^{lo}CD123^+$ and then as $CD34^+CD117^+$.

Adaptive panel

Upon gating on CD45$^+$ hematopoietic cells and the exclusion of doublets, the innate compartment (CD14, CD16 and CD66b) was excluded from the viable cell population. CD3 / CD19 gating allowed the discrimination of B (CD19$^+$) and T (CD3$^+$) cells (Figure 1C).

T cells were further segregated into TCR$\gamma\delta$ positive and negative cell populations. TCR$\gamma\delta^-$ were characterized as MAIT cells if positive for MR1 tetramer staining (12) and subsequently defined as CD8$^+$ or CD4$^+$ depending on CD8β and CD4 expression. The non MAIT cells were gated on CD1d to identify NKT cells (CD3$^+$CD1d$^+$) that were further divided into CD8$^+$ and CD4$^+$ NKT cells based on the expression of CD8$^+$ or CD4$^+$ molecules, respectively. The activation status of both NKT and MAIT cells were determined by the expression of HLA-DR molecule.

CD4$^+$ and CD8b$^+$ T cells were gated and analyzed upon exclusion of NKT cells. We characterized naïve (T_N), central memory (T_{CM}), effector memory (T_{EM}) and effector memory expressing RA (T_{EMRA}) subpopulations of both T cell subsets, based on their expression of CD45RA and CD27. Since T_N and T_{CM} cells have also been defined by the expression of CCR7, we assessed the expression of CCR7 by these cell populations. The activation status was additionally established by the expression of HLA-DR, PD1 and CD56 molecules.

Regulatory T cells (Treg) were identified among CD4$^+$ T cells as CD25$^+$CD127$^-$ and subsequently divided into naïve, memory and activated based on CD45RA and HLA-DR expression (CD45RA$^+$HLA-DR$^-$, CD45RA$^-$HLA-DR$^-$, CD45RA$^-$HLA-DR$^+$, respectively). All 3 Treg subpopulations were additionally investigated for expression of the costimulatory molecule ICOS.

CD25$^-$ CD4$^+$ T cells were additionally gated on CD127 and four subpopulations (T_N, T_{CM}, T_{EM} and T_{EMRA}) were identified among CD127+ cells by expression of CD45RA and CD27 (the same gating strategy as for the CD8$^+$ T cells). Expression of CCR7, HLA-DR, PD1, CD56 and CD95 (for T_N) was subsequently determined. In addition, the CD4$^+$ T cell population expressing CD8a was identified. The CD127$^+$ CD4$^+$ T cells expressing the chemoattractant receptor-homologous molecule and/or different chemokine C receptors were identified by two distinct gating strategies: 1) CD45RA$^-$CXCR5$^+$ were gated on CCR6 and CXCR3 and CXCR5$^+$CCR6$^-$ subsequently on CXCR3 and CCR4; 2) CD45RA$^-$CXCR5$^-$ were gated on CCR6 and CXCR5 and CCR6$^-$ cells additionally on CXCR3 and CCR4 with subsequent gating of CCR4$^+$CXCR3$^-$ cells on CRTh2 and CXCR3.

CD19$^+$ B cells were gated on CD27 and IgD to detect CD27$^+$IgD$^+$, CD27$^+$IgD$^-$, CD27$^-$IgD$^+$ and CD27$^-$IgD$^-$ subpopulations. All four subtypes were analyzed for the expression of IgG, IgM and IgA. The CD27$^+$IgD$^-$ memory B cell subtype was furthermore characterized in more detail. Additional gating on CD38 and CD24 allowed segregation of plasmacytes (CD38^{high}), germinal center B cells (CD38^{low}) and marginal zone B cells (CD24$^{+/-}$ CD38$^-$). Marginal zone B cells were further separated into CD24^{high} (CD21$^{+/low}$), CD24^{int} (CD21$^{+/low}$) and CD24^{low} (CD21$^{+/low}$). CD27$^-$IgD$^+$ B cells were additionally gated on CD38 and CD24 to discriminate naïve B cells (CD38$^-$), transitional B cells (CD24$^+$CD38$^+$), and founder B cells (CD38$^-$). CD19$^+$ B cells were furthermore gated for the expression of the chemokine receptor CXCR4.

Assay validation: technical replicates and robustness of the staining procedures

Repeatability

As this protocol has been designed for the study of immunological variance in a large cohort (MI 10-year follow-up study), we needed to define the technical variance in our

immunophenotyping procedures by performing reproducibility and repeatability experiments. To confirm the repeatability, we analyzed the same sample, in five independent runs, by a single operator. In our experimental setting, fresh blood samples from five healthy donors were separated into five aliquots each then processed and stained separately using each panel, as described in the operating procedure. The results of this test for both panels were highly consistent, with intra-panel coefficients of variation (CVs) below 15% for most of the analyzed cell subsets, irrespective of their absolute counts (Figure 2). For the major circulating immune populations, including neutrophils, eosinophils, basophils, monocytes, T cell subsets (Treg, $CD4^+$, $CD8^+$, MAIT), and B cells, CV values were between 1.09% and 9.13% (cell proportions) and between 4.33% and 14.82% (absolute cell numbers). This was the case even for the rare cell populations like cDCs (14.51% and 7.25%, cell proportion and absolute cell number, respectively), pDCs (9.52% and 13.72%, cell proportion and absolute cell number, respectively) and ILCs (11.75% and 11.68%, cell proportion and absolute cell number, respectively).

While the results of the repeatability test demonstrate the robustness of our protocol when applied by the same operator during a given experiment, they do not provide insight for its reliability in a longitudinal study.

Reproducibility

To confirm the robustness of the staining procedures and the stability of staining over time, an important consideration for large cohort studies, we assessed reproducibility of our assays. To provide a stable reference, we utilized commercially available stabilized human blood (CD-Chex Plus BD, Eurobio Scientific) that was analyzed in five independent experiments, across a 2-week period (Figure 3). These data showed reproducible results with CVs under 13% for proportions of NK cells (4.37%), monocytes (7.64%), ILCs (12.44%) and neutrophils (3.55%), and CVs under 15% for proportions of B cells (14.30%) and T cell subsets (TCR$\gamma\delta$ (9.03%), $CD4^+$ (3.64%), $CD8^+$ (3.93%)).

These results provide evidence that our protocol for staining of fresh blood is highly standardized and could be applied to long-term clinical or translational studies that require multiple sample collections and analyses over a longer period of time.

Fresh blood vs PBMCs

For certain studies and clinical trials, accessibility of fresh whole blood for flow cytometry analysis can be logistically challenging. The most common solution is density gradient centrifugation and isolation of peripheral blood mononuclear cells (PBMCs) and subsequent freezing, which can introduce technical variability (13) and remove important immune cell subsets (e.g. granulocytes). More recent technical solutions (e.g. Cytodelics, SMART tube) allow freezing of whole blood for later analysis (14). Given our interest to phenotype granulocytes, removed during PBMC isolation, we tested the Cytodelics blood stabilization kit. Unfortunately, the fixation led to loss of signal for certain antibodies, likely due to conformational changes of targeted epitopes (Supplementary table 3). Given the necessity of some studies to work with PBMCs, we also tested our panels on freshly isolated PBMCs and PBMCs preserved in CellCover solution and compared the results with those of fresh whole blood from the same

donors, obtained in the same experimental setup. The comparison was made between 200µl of fresh blood, 1 million PBMCs and 0.2 million PBMCs. While 0.2 million PBMCs correspond to the estimated number of PBMCs in 200µl of fresh blood, a sample with 1 million PBMCs was included to allow the detection of minor and rare cell populations or phenotypes with higher precision. This also allowed us to test our staining conditions with 5-fold superior cell numbers compared to what it was originally developed for, and to confirm that our panels and staining procedures work equally well with a broad range of samples.

As can be seen in Figure 4, the percentage of viable cells and absolute cell numbers between whole blood and corresponding PBMCs were comparable for both panels. As expected, the percentage of viable B and T cells was higher in PBMCs than in corresponding whole blood (Figure 4A), while the absolute cell numbers were not significantly different (Figure 4B). Certain differences were observed for NKT, Treg and TCR$\gamma\delta$ cells, which might be due to low population proportions and/or cell numbers. Regarding the innate panel, as expected, neutrophils and eosinophils were well detected in whole blood and, to a lesser extent in PBMCs (Figure 4C-D), whereas the percentage of viable basophils was higher in PBMCs than in whole blood (Figure 4C). This was not the case when absolute numbers were compared (Figure 4D). The proportion of NK cells, monocytes, cDCs, pDCs, and ILCs among the viable cells were at comparable levels (Figure 4C), while absolute numbers for NK cells, cDCs, and pDCs were significantly higher in fresh blood (Figure 4D). This could be explained by cell loss during the PBMC isolation procedure, which may be higher for rare cell populations.

The validation in both fresh blood and PBMCs confirms the potential of our protocols and panels for application in a wide variety of human-based studies.

Semi-automation

The implementation of automated procedures can help to eliminate possible errors or variation caused by repetitive work during a prolonged period by technical personnel, which is particularly relevant for clinical studies with large sample numbers. Therefore, we took advantage of automation in sample preparation for our standardized cellular immunophenotyping protocol. To achieve this, we implemented our protocol using the Freedom EVO150 liquid handling platform (Tecan). The premix of antibodies was prepared manually on a daily basis, and all other steps for the sample preparation and staining protocol were performed using the liquid handling platform, EVO150, with the exception of centrifugation. The pipetting scripts for the platform were created to enable the staining of 10 samples, in parallel, in 5 ml round bottom tubes. The script is available at https://github.com/cbutechs/MI_spectral. The automation process requires validation prior to implementation in clinical studies. To this end, one operator performed a repeatability assay within a single day manually and with the automation platform in parallel. One whole-blood sample from a healthy donor was divided into ten aliquots and immediately processed and stained in parallel (5 manually, 5 automated). Results from representative analysis of three experiments are shown in Figure 5. For all analyzed immune cell populations, no significant difference between absolute cell numbers was observed, when comparing manual experimentation with the semi-automated platform. This was the case for major cell populations such as B cells (P=0.0625), T cells (P=0.1250), neutrophils (P=0.1875), monocytes (P=0.6250), but also for minor immune cell populations

such as pDCs (P=0.6250), ILCs (P=0.6250), MAIT cells (P=0.1250), NKT cells (P=0.0625) and Treg (P>0.9999).

Standardized semi-automation of our protocol further facilitates its implementation in large-cohort clinical studies where there is a real risk of a technical variability introduced by repetitive manual work.

Unsupervised data analysis

Analysis of high-dimensional flow cytometry data is the major challenge of advanced cell phenotyping. In addition to manual data analysis by FlowJo, we employed an unsupervised approach to visualize major cell subsets identified by innate and adaptive panels in one donor. We used a prototype of Sony data analysis software that relies on algorithms like Flt-sne, UMAP and flowAI incorporated in the native prototype Sony Software. The software uses the original Sony ID7000 format files instead of FCS. As shown in Figure 6A, this unsupervised approach allowed to identify the major innate and adaptive immune subsets previously characterized by the supervised analysis.

We are currently testing different tools for unsupervised analysis to identify the most appropriate solution for an in-depth characterization of the cell phenotypes that can be revealed by our panels.

Application to phenotyping of samples from patients with autoimmune / autoinflammatory diseases

We have developed our panels and protocol with the aim of rendering them applicable for in-depth cellular phenotyping in the context of a wide variety of translational and clinical studies. Therefore, it was important to confirm that our panels and methods are sensitive enough to capture differences in immune cell phenotypes between healthy subjects and subjects with pathological conditions. For this proof-of-concept application, we compared a small number of patients with different autoimmune/autoinflammatory diseases (n=8) (Supplementary table 4) with age and sex matched healthy donors (n=8). We proceeded with the data analysis of these samples in two steps.

First, we performed an unsupervised analysis of one patient with inflammatory disease and one age/sex-matched healthy subject to visualize the distribution of major immune cell subsets between these two individuals. The Flt-sne representation of data upon unsupervised analysis after staining with the innate panel (Figure 6B) indicated a distinct neutrophil distribution between healthy and patient samples, suggesting phenotypic variance within this cell population. Similarly, there was an evident discrepancy in the distribution of $CD8^+$, $CD4^+$ and $CD19^+$ cell subsets (Figure 6C). A more detailed unsupervised analysis showed clear differences between the patient and the healthy donor for $CD4^+$ T cells (naïve, CM, EM, EMRA) (Supplementary figure 2A), $CD4^+$ T cell subsets (Th, Treg, MAIT) (Supplementary figure 2B), $CD8^+$ T cells (naïve, CM, EM, EMRA) (Supplementary figure 2C) and B cell subsets (Supplementary figure 2D).

To confirm that discrepancies between the healthy and the diseased subject were not a result of technical bias introduced by the unsupervised analysis tool, we performed manual characterization of these two samples. As shown in Figure 6C there were obvious differences between major innate immune cell populations (e.g., neutrophils, eosinophils, monocytes, NK cells), in line with the tSNE representation upon unsupervised analysis. Similarly, the major

adaptive cell subsets were found in significantly different proportions in the patient versus healthy sample (Figure 6D).

In the second step, we have analyzed the data of all eight patients and their matched healthy controls by supervised analysis to compare a total of 182 cell phenotypes. We found that 16 minor/rare cell populations including NKT, $CD1c^+$ cDCs, MAIT and $IgG^+IgM^+CD27^-IgD^+$cells show significant differences with an uncorrected p value of <0.05 (Figure 6E). Four of these, all related to B cell subsets, remained significant even after correcting for multiple testing.

We have not further explored the observed differences since it was out of the scope of this work, and we had too small sample size for tackling in depth questions. Nevertheless, this validation step confirmed the advantage and suitability of our protocol for clinical trials or studies that require the detection of minor changes of rare immune cell populations and their phenotypes introduced by different pathological environments.

DISCUSSION

Multi-parameter flow cytometry is a powerful technique that allows deep characterization of immune cell subpopulations in clinical and translational studies. However, a major challenge is the correct choice of tools and techniques that allow reliable and performant comparison between individual subjects and across different studies. To this end, the standardization and development of robust protocols is of the highest importance, as underlined by various recent publications (15–18).

In 2011, we developed a standardized procedure for flow cytometry allowing us to analyze the 1,000 healthy donors of the *Milieu Intérieur* study. To analyze major immune phenotypes and considering the technological advances at that time, we established a standardized staining protocol with 10 separate panels. Over the past years, flow cytometry technologies have significantly improved, resulting in the development of new, more powerful cytometers such as spectral cytometry, first commercialized by Sony Biotechnology (10). The simultaneous development of new reagents, monoclonal antibodies, and a variety of new fluorochromes allowed us to replace ten 8-color panels with two 35-34-color panels. Consequently, the benefit is multiple: a) decrease in required sample volume, b) considerable time reduction and therefore c) cost reduction.

Initially, we considered the CytoFLEX (Beckman Coulter) and Symphony A5 (BD Bioscience) flow cytometers for this project and performed the initial testing of panels on these machines. However, the obtained results were not satisfactory. Although equipped with a deep-well plate reader, CytoFLEX was limited by low dimensionality. The high dimensionality of our panels rendered the complexity of panel design that was challenging for the Symphony A5. In addition, the instrument lacked the possibility to perform the acquisition from Deepwell plates.

Nowadays, spectral flow cytometers are heavily used in the field of immunology, where there is a need for simultaneous analysis of as many cell markers as possible to characterize different immune cell populations and their phenotypes (11). The ID7000 instrument (Sony Biotechnology) that we chose for the study is a cutting-edge spectral technology, well-adapted to our study, with one limitation, the lack of automated cell counting. While in the initial MI study we relied on a cytometer that had a cell counting capacity, here, we were dependent on the

use of counting beads to assess absolute cell numbers. This resulted in less satisfying CVs for the reproducibility and repeatability tests, in particular for minor/rare immune cell subsets.

The major challenge of high-dimensional flow cytometry (conventional and spectral) remains data analysis. It starts with compensations in the case of conventional cytometry, and with spectral signal unmixing in spectral cytometry. Both have a significant impact on the results and reproducibility. The manual unmixing and its adjustments is both time-consuming and biased by its manual nature. The proprietary data format for the raw data makes finding automated procedures challenging. Traditional analysis using 1 and 2 dimensional gates is usually done manually and is difficult to reproduce (19). While the gold standard FlowJo approach is convenient for defining an initial gating strategy, application of an unsupervised data analysis pipeline is better suited for the large number of measured parameters (>35) and for the analysis of numerous samples in clinical studies (20). The unsupervised approach allows identification of novel cellular clusters, without prior knowledge of their characteristics, potentially leading to the discovery of previously uncharacterized immune cell populations and their roles in various disease states. Most methods and workflows currently rely on self-organizing maps (KOHONEN)(21) like FlowSOM (22,23) or Catalyst (24). Several pipelines for unsupervised analysis are commercially available (e.g. OMIQ, Tercen, Ozette, METAFORA, FCS express, Cytobank, FlowJo plugins), but all show certain limitations. Unsupervised, similar to supervised pipelines, imply the choice of transformation and optimization of its parameters (biexponential versus inverse hyperbolic sine (asinh)), for which there is still no consensus in the community. When dealing with human samples, due to the large variability of data, spectra need to be aligned, which complicates the analysis of fluorescent shift. The key is to ensure that the applied method is reproducible and thus adapted to further studies.

The major added value of a standardized protocol like ours is its versatility. We have demonstrated its applicability in the analysis of both fresh blood and PBMCs, which renders it beneficial for a vast range of studies and clinical trials. In addition, we have demonstrated the capacity of our approach to identify small shifts in cell phenotypes in pathological conditions, by applying it to the analysis of samples from a small cohort of patients with autoimmune/inflammation diseases and comparing them to sex/age-matched healthy donors from MI 10-year follow-up study. The obtained results confirm the capacity of our protocol to detect changes (even) in rare, minor cell populations.

In summary, our standardized protocol and two high-dimensional spectral cytometry panels are well-adapted to immunomonitoring in a wide range of clinical studies based on analysis of fresh blood and/or PBMC.

MATERIALS and METHODS

Healthy donors

Fresh whole blood was collected from healthy French volunteers enrolled at the Clinical Investigation and Access to BioResources (ICAReB) platform (Center for Translational Research, Institut Pasteur, Paris, France). These donors were part of the CoSImmGEn cohort (NCT03925272). Additional blood was obtained from donors recruited as part of the Milieu

Interieur 10 year longitudinal V3 study (NCT05381857) performed at Biotrial, Rennes. This clinical study was approved by the CPP (Comités de Protection des Personnes) Nord Ouest III and ANSM (Agence nationale de sécurité du médicament et des produits de santé). Written informed consent was obtained from all study participants. Stabilized whole blood was obtained from Streck (350174/39).

Patient samples

Human patient samples were collected in Cochin Hospital (Paris, France), in the setting of the local RADIPEM biological samples collection derived from samples collected in routine care. Biological collection and informed consent were approved by the Direction de la Recherche Clinique et Innovation (DRCI) and the French Ministry of Research (N°2019-3677).

Sample preparation

Whole blood was collected on Li-heparin as anti-coagulant and maintained at 18–25°C until processing (6 to 8 h). To eliminate soluble antibodies and other molecules that may interfere with staining, 1 ml of whole blood was washed by mixing fresh whole blood and PBS at a ratio of 1:1, followed by centrifugation at 500 g for 5 min at 18-22°C (room temperature, RT). The supernatant was discarded, PBS was added up to 1 ml and shortly vortexed.

Staining protocol

Washed blood (200 µl per staining panel) was added to Live/dead solution to obtain 1:1000 Live/dead final dilution and incubated for 30 min at RT protected from light. Thereafter, 2 ml of PBS were added to the tubes, centrifuged for 5 min at 500 g, and the supernatant was discarded.

Antibody premixes were prepared, shortly vortexed, spun for 10 s, and added on the surface of the blood pellet. The samples were shortly vortexed and incubated for 20 min at RT, protected from light. 2 ml of PBS were added to the tubes, centrifuged for 5 min at 500 g, and the supernatant was discarded.

All samples were resuspended in 4 ml of RBC lysing solution (BD FACS Lysing Solution, BD Biosciences), vortexed and incubated for 15 min at RT protected from light. Of note, BD FACS Lysing Solution also contains a fixative reagent. Following centrifugation (5 min at 500 g), the supernatant was discarded, the samples were resuspended in 2 ml of PBS to stop the reaction. Upon centrifugation for 5 min at 500 g, the supernatant was discarded, the samples were resuspended in 250 µl PBS, transferred to a 500 µl Deepwell plate and stored at 4°C until acquisition (overnight), protected from light.

Sample acquisition

Before sample acquisition, the ID7000 cytometer was calibrated using fluorescent calibration beads according to the manufacturer's instructions. An acquisition template was created for each panel. Spectral cytometry does not require compensation but does require single stained controls to allow unmixing of obtained data. To this purpose we used OneComp eBeads (eBioscience, ThermoFischer) or single stained cells. The latter were used for tetramers and live/dead marker. The unstained sample was used for measurement of the background signal.

Prior the acquisition, counting beads (123count eBeads, ThermoFischer) were vortexed for 30 s and 50µl were added to each sample.

To ensure the reproducibility of the protocol, the samples were manually mixed just before the acquisition. In addition, the same order of acquisition of the two panels was executed (innate panel first). For each panel, the acquisition of samples was followed by that of unstained control, and of single-stained controls. To avoid cross-contamination, an additional Priming/Washing step was systematically performed between the acquisition of the two panels. The samples were acquired at a speed of around 100 µl per minute, which represented a good compromise between the number of acquired cells, the acquisition time (3 min), the abort and the saturation rate. The dead volume was between 30 and 50 µl.

A delay of 5 s between the beginning of aspiration and start of sample recording ensured recording of data with stable acquisition rate.

Data analysis

Spectral cytometry data were generated using ID7000 software version 1.1.12.25251 and saved in exdat format (SONY). The spectral data were unmixed using the WLSM algorithm of ID7000 software. Then, the unmixed sample data were converted to FCS files and analysed using FlowJo version 10.9 software. Statistical graphs were prepared using Graphpad Prism software version 9.5.1.

The Milieu Intérieur Consortium is composed of the following team leaders: Laurent Abel (Hôpital Necker), Andres Alcover, Hugues Aschard, Philippe Bousso, Nollaig Bourke (Trinity College Dublin), Petter Brodin (Karolinska Institutet), Pierre Bruhns, Nadine Cerf-Bensussan (INSERM UMR 1163 – Institut Imagine), Ana Cumano, Caroline Demangel, Christophe d'Enfert, Ludovic Deriano, Marie-Agnès Dillies, James Di Santo, Gérard Eberl, Jost Enninga, Jacques Fellay (EPFL, Lausanne), Ivo Gomperts-Boneca, Milena Hasan, Magnus Fontes (Institut Roche), Gunilla Karlsson Hedestam (Karolinska Institutet), Serge Hercberg (Université Paris 13), Molly A. Ingersoll (Institut Pasteur and Institut Cochin), Rose Anne Kenny (Trinity College Dublin), Olivier Lantz (Institut Curie), Mickael Ménager (INSERM UMR 1163 – Institut Imagine), Frédérique Michel, Hugo Mouquet, Cliona O'Farrelly (Trinity College Dublin), Etienne Patin, Sandra Pellegrini, Stanislas Pol (Hôpital Côchin), Antonio Rausell (INSERM UMR 1163 – Institut Imagine), Frédéric Rieux-Laucat (INSERM UMR 1163 – Institut Imagine), Lars Rogge, Anavaj Sakuntabhai, Olivier Schwartz, Benno Schwikowski, Spencer Shorte, Frédéric Tangy, Antoine Toubert (Hôpital Saint-Louis), Mathilde Touvier (Université Paris 13), Marie-Noëlle Ungeheuer, Christophe Zimmer, Matthew L. Albert (Hibio), Darragh Duffy, and Lluis Quintana-Murci. Unless otherwise indicated, partners are located at Institut Pasteur, Paris. Darragh Duffy and Lluis Quintana-Murci are co-coordinators of the Milieu Intérieur Consortium.

Acknowledgements

We thank the ICAReB platform of the Institut Pasteur for healthy donor's fresh blood samples. We thank BD for providing the antibodies for testing and NIH Tetramer Core Facility for providing the tetramers used in the study. The MR1 tetramer technology was developed jointly

by Dr. James McCluskey, Dr. Jamie Rossjohn, and Dr. David Fairlie, and the material was produced by the NIH Tetramer Core Facility as permitted to be distributed by the University of Melbourne. This work benefited from support of the French government's Invest in the Future Program, managed by the Agence Nationale de la Recherche (ANR, reference 10-LABX-69-01).

REFERENCES

1. Maecker HT, McCoy JP, Nussenblatt R. Standardizing immunophenotyping for the Human Immunology Project. Nat Rev Immunol 2012;12:191–200.
2. Poland GA, Quill H, Togias A. Understanding the human immune system in the 21st century: The Human Immunology Project Consortium. Vaccine 2013;31:2911–2912.
3. Anon. Action BM0907. COST. Available at: https://www.cost.eu/actions/BM0907. Accessed May 30, 2023.
4. Anon. 10kimmunomes - Default. Available at: https://comphealth.ucsf.edu/app/10kimmunomes. Accessed May 30, 2023.
5. Pappalardo JL, Hafler DA. The Human Functional Genomics Project: Understanding Generation of Diversity. Cell 2016;167:894–896.
6. Orrù V, Steri M, Sole G, Sidore C, Virdis F, Dei M, Lai S, Zoledziewska M, Busonero F, Mulas A, Floris M, Mentzen WI, Urru SAM, Olla S, Marongiu M, Piras MG, Lobina M, Maschio A, Pitzalis M, Urru MF, Marcelli M, Cusano R, Deidda F, Serra V, Oppo M, Pilu R, Reinier F, Berutti R, Pireddu L, Zara I, Porcu E, Kwong A, Brennan C, Tarrier B, Lyons R, Kang HM, Uzzau S, Atzeni R, Valentini M, Firinu D, Leoni L, Rotta G, Naitza S, Angius A, Congia M, Whalen MB, Jones CM, Schlessinger D, Abecasis GR, Fiorillo E, Sanna S, Cucca F. Genetic Variants Regulating Immune Cell Levels in Health and Disease. Cell 2013;155:242–256.
7. Thomas S, Rouilly V, Patin E, Alanio C, Dubois A, Delval C, Marquier L-G, Fauchoux N, Sayegrih S, Vray M, Duffy D, Quintana-Murci L, Albert ML, Milieu Intérieur Consortium. The Milieu Intérieur study - an integrative approach for study of human immunological variance. Clin Immunol 2015;157:277–293.
8. Hasan M, Beitz B, Rouilly V, Libri V, Urrutia A, Duffy D, Cassard L, Di Santo JP, Mottez E, Quintana-Murci L, Albert ML, Rogge L, Milieu Intérieur Consortium. Semi-automated and standardized cytometric procedures for multi-panel and multi-parametric whole blood immunophenotyping. Clin Immunol 2015;157:261–276.
9. Patin E, Hasan M, Bergstedt J, Rouilly V, Libri V, Urrutia A, Alanio C, Scepanovic P, Hammer C, Jönsson F, Beitz B, Quach H, Lim YW, Hunkapiller J, Zepeda M, Green C, Piasecka B, Leloup C, Rogge L, Huetz F, Peguillet I, Lantz O, Fontes M, Di Santo JP, Thomas S, Fellay J, Duffy D, Quintana-Murci L, Albert ML, Milieu Intérieur Consortium. Natural variation in the parameters of innate immune cells is preferentially driven by genetic factors. Nat Immunol 2018;19:302–314.
10. Vorobjev IA, Kussanova A, Barteneva NS. Development of Spectral Imaging Cytometry. In: Barteneva NS, Vorobjev IA, editors Spectral and Imaging Cytometry: Methods and Protocols. Methods in Molecular Biology. New York, NY: Springer US; 2023. p 3–22. Available at: https://doi.org/10.1007/978-1-0716-3020-4_1. Accessed May 30, 2023.
11. Futamura K, Sekino M, Hata A, Ikebuchi R, Nakanishi Y, Egawa G, Kabashima K, Watanabe T, Furuki M, Tomura M. Novel full-spectral flow cytometry with multiple spectrally-adjacent fluorescent proteins and fluorochromes and visualization of in vivo cellular movement. Cytometry Part A 2015;87:830–842.
12. Corbett AJ, Eckle SBG, Birkinshaw RW, Liu L, Patel O, Mahony J, Chen Z, Reantragoon R, Meehan B, Cao H, Williamson NA, Strugnell RA, Van Sinderen D, Mak JYW, Fairlie DP, Kjer-Nielsen L, Rossjohn J, McCluskey J. T-cell activation by transitory neo-antigens derived

from distinct microbial pathways. Nature 2014;509:361–365.
13. Brodin P, Duffy D, Quintana-Murci L. A Call for Blood-In Human Immunology. Immunity 2019;50:1335–1336.
14. Henrick BM, Rodriguez L, Lakshmikanth T, Pou C, Henckel E, Arzoomand A, Olin A, Wang J, Mikes J, Tan Z, Chen Y, Ehrlich AM, Bernhardsson AK, Mugabo CH, Ambrosiani Y, Gustafsson A, Chew S, Brown HK, Prambs J, Bohlin K, Mitchell RD, Underwood MA, Smilowitz JT, German JB, Frese SA, Brodin P. Bifidobacteria-mediated immune system imprinting early in life. Cell 2021;184:3884-3898.e11.
15. Cossarizza A, Chang H-D, Radbruch A, Akdis M, Andrä I, Annunziato F, Bacher P, Barnaba V, Battistini L, Bauer WM, Baumgart S, Becher B, Beisker W, Berek C, Blanco A, Borsellino G, Boulais PE, Brinkman RR, Büscher M, Busch DH, Bushnell TP, Cao X, Cavani A, Chattopadhyay PK, Cheng Q, Chow S, Clerici M, Cooke A, Cosma A, Cosmi L, Cumano A, Dang VD, Davies D, De Biasi S, Del Zotto G, Della Bella S, Dellabona P, Deniz G, Dessing M, Diefenbach A, Di Santo J, Dieli F, Dolf A, Donnenberg VS, Dörner T, Ehrhardt GRA, Endl E, Engel P, Engelhardt B, Esser C, Everts B, Dreher A, Falk CS, Fehniger TA, Filby A, Fillatreau S, Follo M, Förster I, Foster J, Foulds GA, Frenette PS, Galbraith D, Garbi N, García-Godoy MD, Geginat J, Ghoreschi K, Gibellini L, Goettlinger C, Goodyear CS, Gori A, Grogan J, Gross M, Grützkau A, Grummitt D, Hahn J, Hammer Q, Hauser AE, Haviland DL, Hedley D, Herrera G, Herrmann M, Hiepe F, Holland T, Hombrink P, Houston JP, Hoyer BF, Huang B, Hunter CA, Iannone A, Jäck H-M, Jávega B, Jonjic S, Juelke K, Jung S, Kaiser T, Kalina T, Keller B, Khan S, et al. Guidelines for the use of flow cytometry and cell sorting in immunological studies. Eur J Immunol 2017;47:1584–1797.
16. Cossarizza A, Chang H-D, Radbruch A, Acs A, Adam D, Adam-Klages S, Agace WW, Aghaeepour N, Akdis M, Allez M, Almeida LN, Alvisi G, Anderson G, Andrä I, Annunziato F, Anselmo A, Bacher P, Baldari CT, Bari S, Barnaba V, Barros-Martins J, Battistini L, Bauer W, Baumgart S, Baumgarth N, Baumjohann D, Baying B, Bebawy M, Becher B, Beisker W, Benes V, Beyaert R, Blanco A, Boardman DA, Bogdan C, Borger JG, Borsellino G, Boulais PE, Bradford JA, Brenner D, Brinkman RR, Brooks AES, Busch DH, Büscher M, Bushnell TP, Calzetti F, Cameron G, Cammarata I, Cao X, Cardell SL, Casola S, Cassatella MA, Cavani A, Celada A, Chatenoud L, Chattopadhyay PK, Chow S, Christakou E, Čičin-Šain L, Clerici M, Colombo FS, Cook L, Cooke A, Cooper AM, Corbett AJ, Cosma A, Cosmi L, Coulie PG, Cumano A, Cvetkovic L, Dang VD, Dang-Heine C, Davey MS, Davies D, De Biasi S, Del Zotto G, Dela Cruz GV, Delacher M, Della Bella S, Dellabona P, Deniz G, Dessing M, Di Santo JP, Diefenbach A, Dieli F, Dolf A, Dörner T, Dress RJ, Dudziak D, Dustin M, Dutertre C-A, Ebner F, Eckle SBG, Edinger M, Eede P, Ehrhardt GRA, Eich M, Engel P, et al. Guidelines for the use of flow cytometry and cell sorting in immunological studies (second edition). Eur J Immunol 2019;49:1457–1973.
17. McCausland M, Lin Y-D, Nevers T, Groves C, Decman V. With great power comes great responsibility: high-dimensional spectral flow cytometry to support clinical trials. Bioanalysis 2021;13:1597–1616.
18. Kalina T. Reproducibility of Flow Cytometry Through Standardization: Opportunities and Challenges. Cytometry A 2020;97:137–147.
19. Maecker HT, Rinfret A, D'Souza P, Darden J, Roig E, Landry C, Hayes P, Birungi J, Anzala O, Garcia M, Harari A, Frank I, Baydo R, Baker M, Holbrook J, Ottinger J, Lamoreaux L, Epling CL, Sinclair E, Suni MA, Punt K, Calarota S, El-Bahi S, Alter G, Maila H, Kuta E, Cox J, Gray C, Altfeld M, Nougarede N, Boyer J, Tussey L, Tobery T, Bredt B, Roederer M, Koup R, Maino VC, Weinhold K, Pantaleo G, Gilmour J, Horton H, Sekaly RP. Standardization of cytokine flow cytometry assays. BMC Immunol 2005;6:13.
20. Liechti T, Weber LM, Ashhurst TM, Stanley N, Prlic M, Van Gassen S, Mair F. An updated guide for the perplexed: cytometry in the high-dimensional era. Nat Immunol 2021;22:1190–1197.

21. Kohonen T. The self-organizing map. Proceedings of the IEEE 1990;78:1464–1480.
22. Quintelier K, Couckuyt A, Emmaneel A, Aerts J, Saeys Y, Van Gassen S. Analyzing high-dimensional cytometry data using FlowSOM. Nat Protoc 2021;16:3775–3801.
23. Cheung M, Campbell JJ, Whitby L, Thomas RJ, Braybrook J, Petzing J. Current trends in flow cytometry automated data analysis software. Cytometry A 2021;99:1007–1021.
24. Chevrier S, Crowell HL, Zanotelli VRT, Engler S, Robinson MD, Bodenmiller B. Compensation of Signal Spillover in Suspension and Imaging Mass Cytometry. Cell Systems 2018;6:612-620.e5.

A

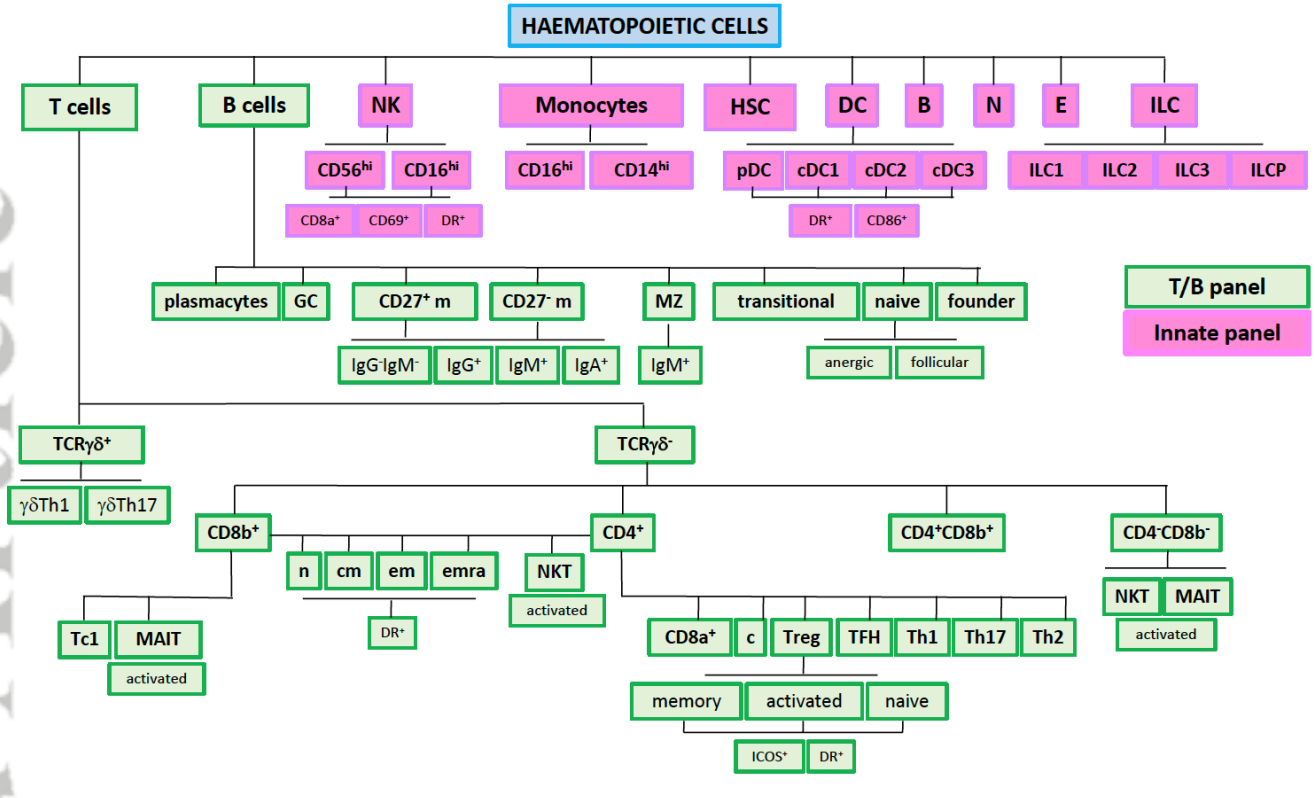

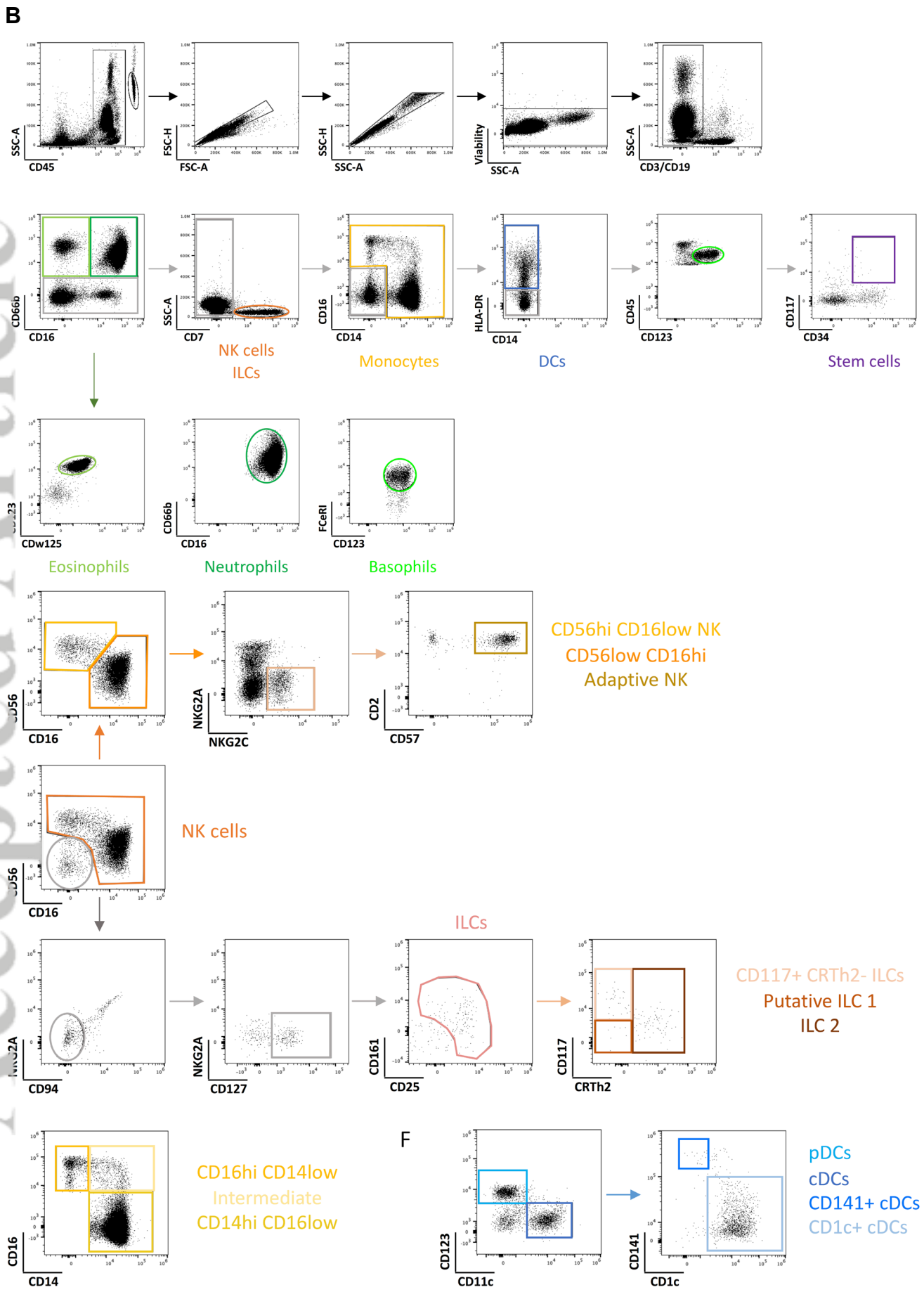

C

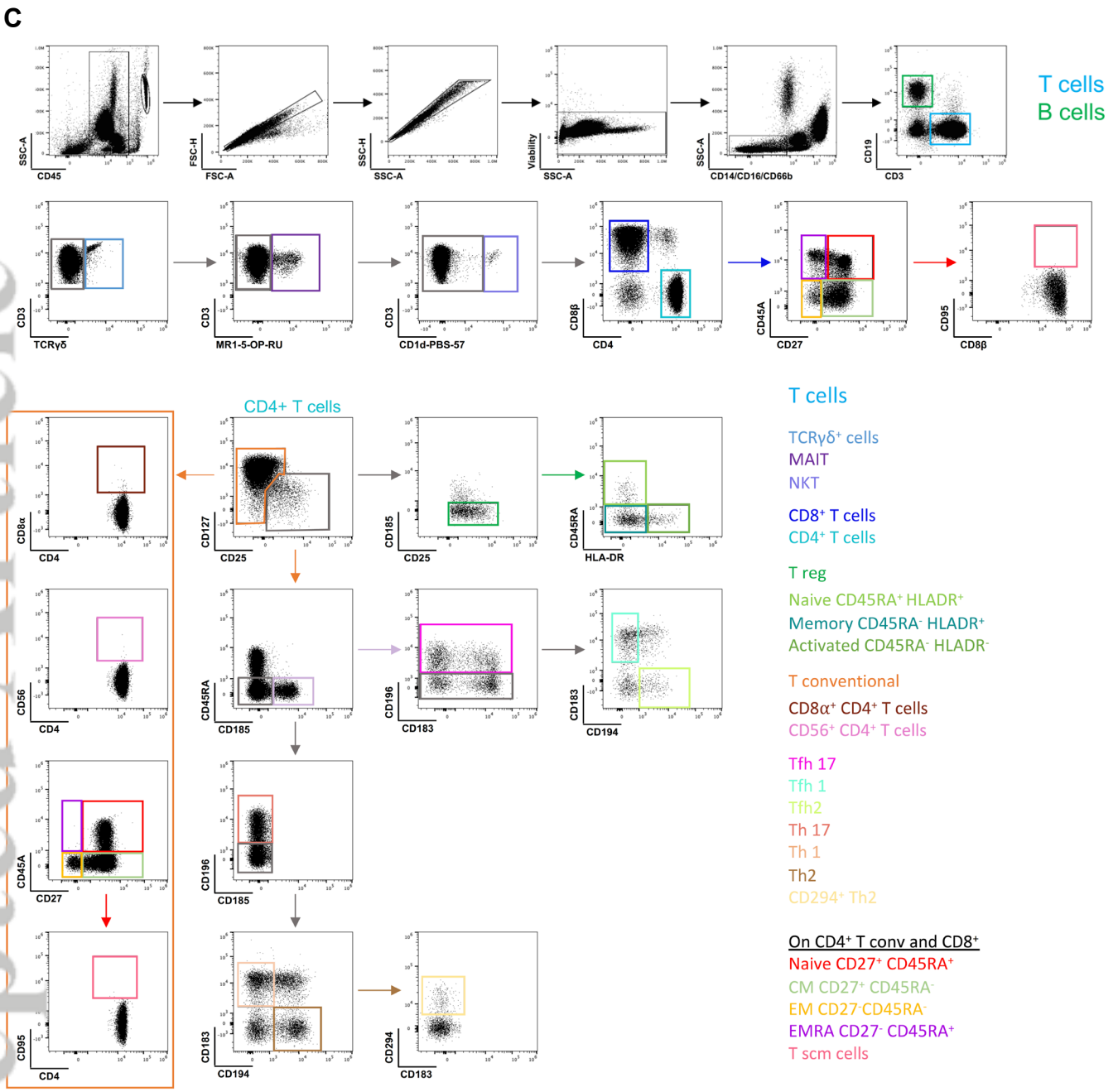

T cells

TCRγδ⁺ cells
MAIT
NKT

CD8⁺ T cells
CD4⁺ T cells

T reg
Naive CD45RA⁺ HLADR⁺
Memory CD45RA⁻ HLADR⁺
Activated CD45RA⁻ HLADR⁻

T conventional
CD8α⁺ CD4⁺ T cells
CD56⁺ CD4⁺ T cells

Tfh 17
Tfh 1
Tfh2
Th 17
Th 1
Th2
CD294⁺ Th2

On CD4⁺ T conv and CD8⁺
Naive CD27⁺ CD45RA⁺
CM CD27⁺ CD45RA⁻
EM CD27⁻CD45RA⁻
EMRA CD27⁻ CD45RA⁺
T scm cells

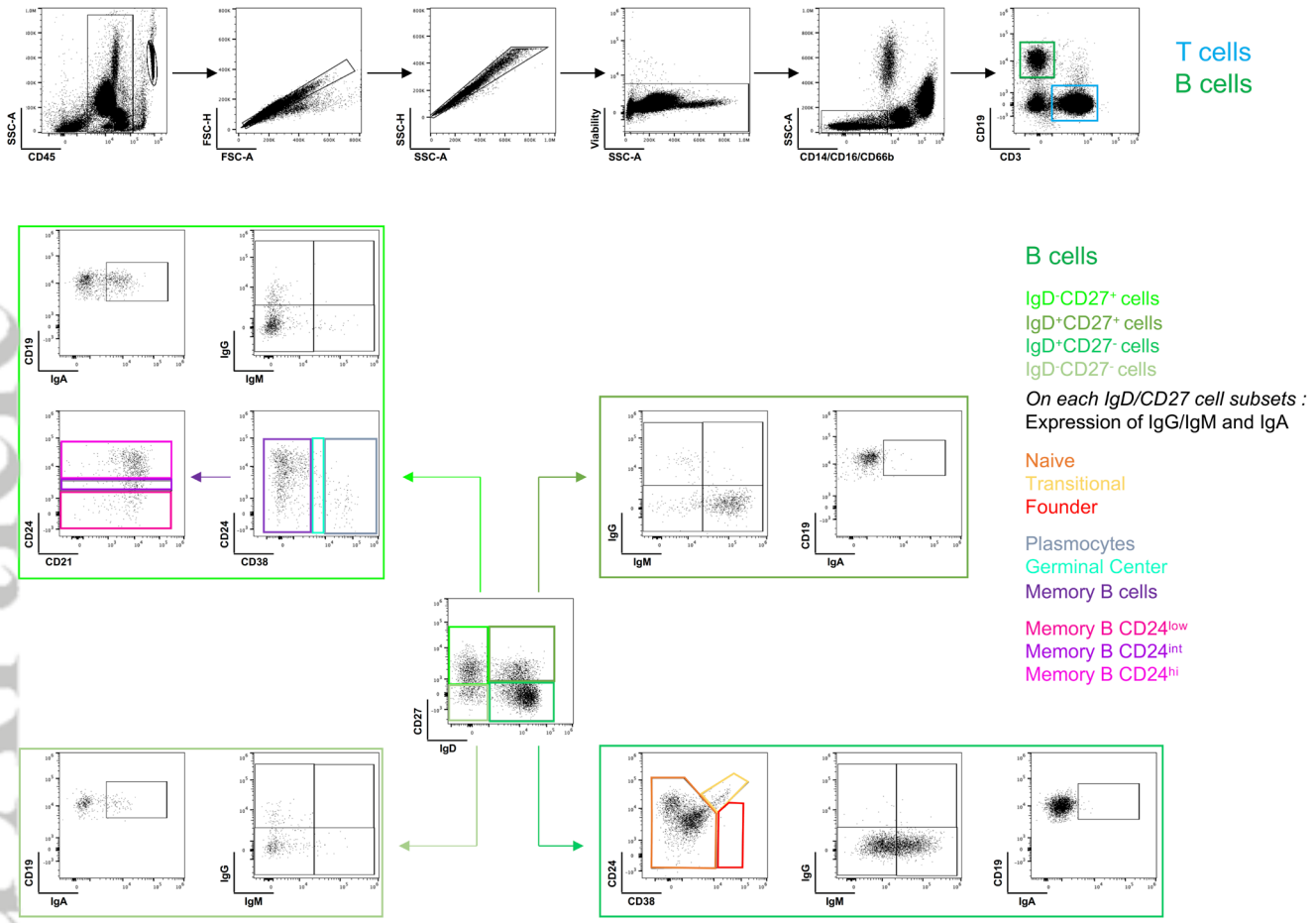

Figure 1. Identification of major innate and adaptive immune cell populations in fresh peripheral blood. A) The scheme represents pre-defined immune cell sub-populations that can be identified. Staining protocol and the choice of antibodies enable identification of 182 immune cell phenotypes. B) Innate immune cell populations were identified as live CD45+ singlet cells after the exclusion of the dump channel ($CD3^+$ and $CD19^+$ cells). Polymorphonuclear (PMN) cells were divided into Eosinophils ($CD123^+$ $CDw125^+$), Neutrophils ($CD66b^+$ $CD16^+$) and Basophils ($FCeRI^+$ $CD123^+$). Upon gating on $CD7^+$ cells, NK and ILCs subpopulations could be described. Monocyte subsets were gated with CD16 and CD14 markers. Different DCs subpopulations were segregated upon CD123, CD11c and CD141, CD1c staining. The activation status of PMNs (CD16, CD32, CD63, CXCR4, FCeRI, HLADR, CD62L and PDL1), NK cells (CD56, CD69, CD8a), monocytes (HLA-DR, CD4, PDL-1) and DCs (CD86, CXCR4, CD4, HLA-DR, PDL-1, CD8a) were assessed (not shown). C) Adaptive cells were identified as live $CD45^+$ singlet cells exempt from $CD14^+$, $CD66b^+$ and $CD16^+$ cells. T and B cells were characterized as $CD3^+$ and $CD19^+$, respectively. The major T cell subpopulations such as $T\gamma\delta$, MAIT, NKT, CD8 and CD4, as well as associated subpopulations (Th and Tfh) were distinguished among $CD3^+$ cells. Within B cells, various markers are used to identify the major B cell sub-populations. The activation status was defined based on the expression of HLA-DR for MAIT and NKT (not shown). The expression of CXCR4, CD8a, CCR7, HLA-DR, PD1, CD95, ICOS and CD56 was used for additional characterization of T cell subsets (not shown).

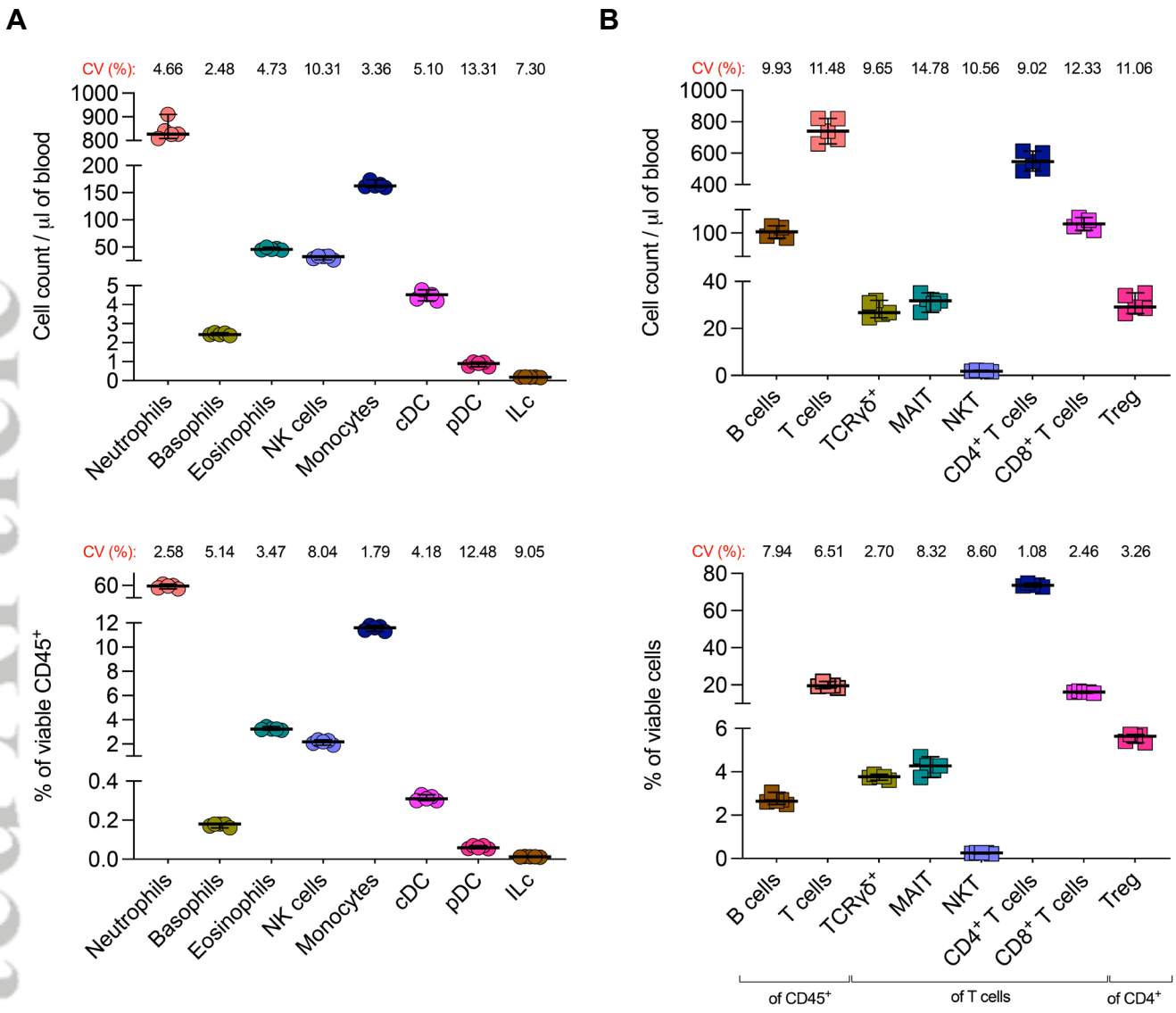

Figure 2. Repeatability study using fresh whole blood. Fresh blood samples of a donor were aliquoted in five tubes with 200 µl of blood, processed and stained by innate and adaptive panels, as described. This was done for five donors in total. Numbers (upper panels) and proportions (lower panels) of selected innate (A) and adaptive (B) cell subsets are shown. The CVs for serial measurements are indicated for each analyzed immune cell population.

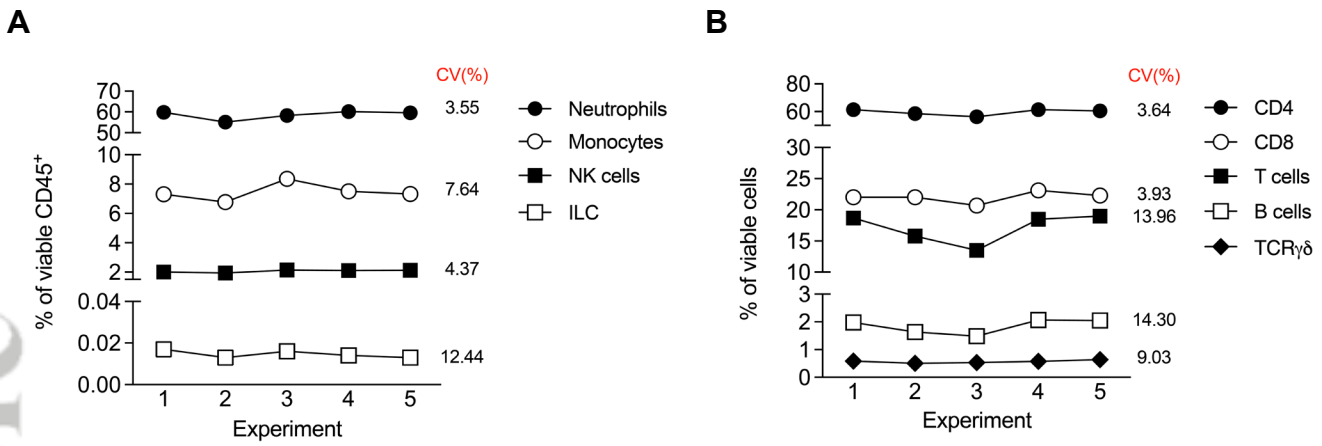

Figure 3. Reproducibility assay using commercially available stabilized blood. Stabilized human blood (CD-Chex Plus, Eurobio Scientific) was analyzed in five independent experiments, across a 2-week period. The percentages of indicated cell subsets for (A) innate and (B) adaptive panels are shown. The CVs for serial measurements are indicated for each analyzed immune cell population.

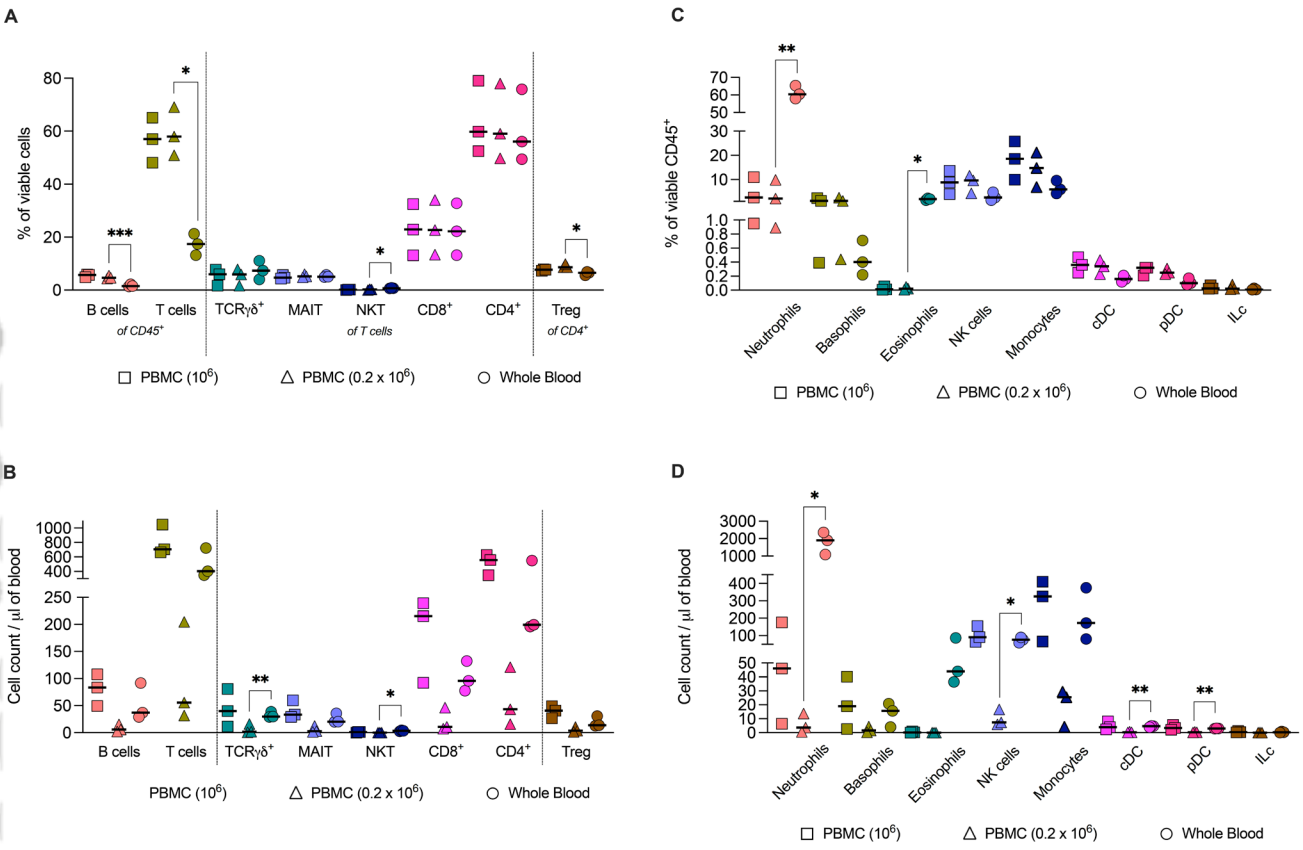

Figure 4. Fresh blood vs PBMC comparison. A part of fresh blood from 3 donors was used for PBMC isolation. Both fresh blood and the corresponding PBMCs were analyzed in a single experiment. The percentages of indicated cell subsets for (A) adaptive and (C) innate panels and absolute cell numbers for (B) adaptive and (D) innate panels are shown. The significant difference between 0.2 million PBMCs and fresh blood was expressed by the *. *P* values were calculated by paired t-test. *, P<0.05; **, P<0.005; ***, P<0.0005.

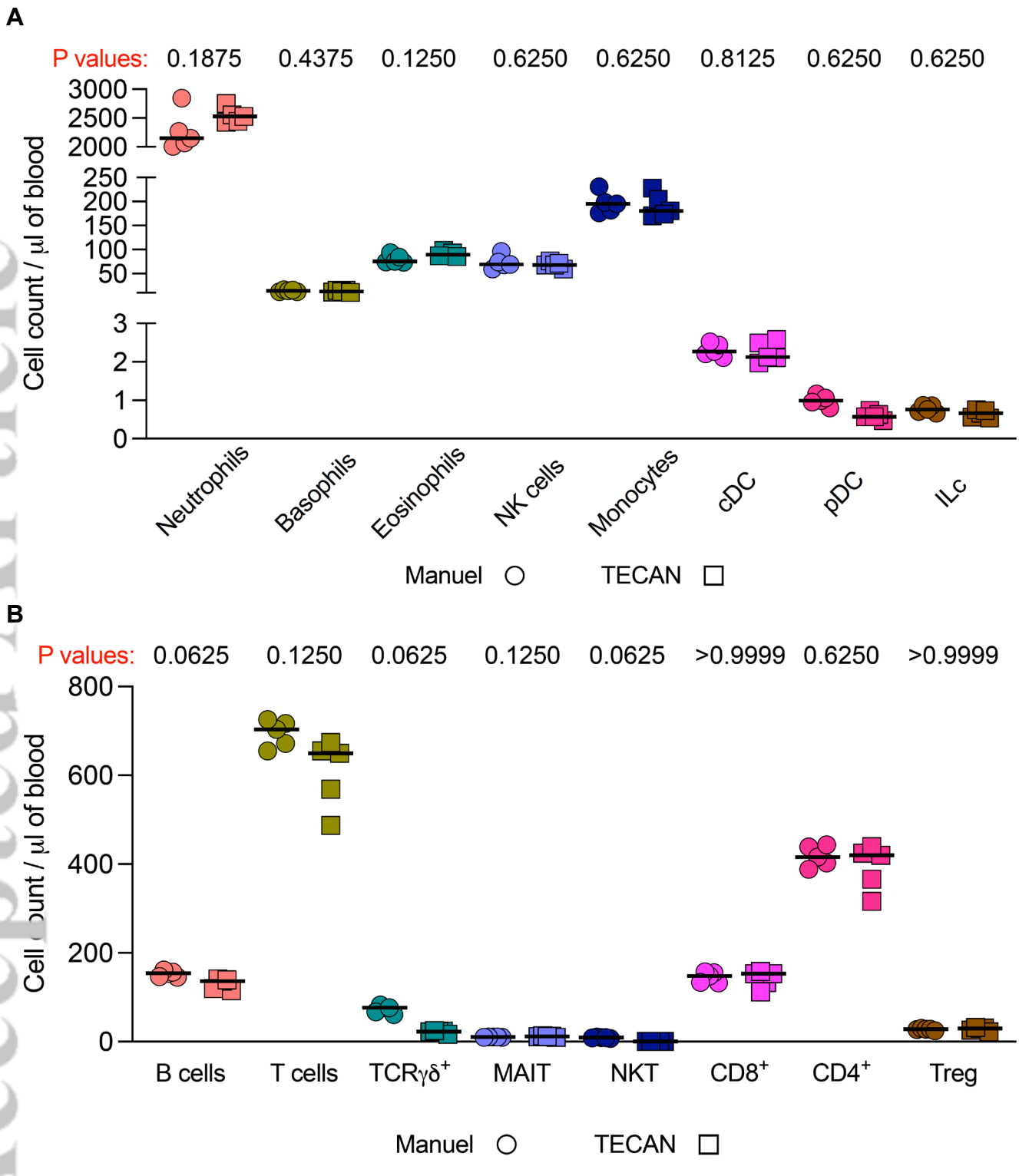

Figure 5. Semi-automation of sample processing and staining of whole blood. Fresh blood samples of a donor were aliquoted in five tubes with 200 µl of blood, processed and stained by innate and adaptive panels, manually and with automated platform in parallel. This was performed for three donors. Numbers of selected innate (A) and adaptive (B) cell subsets are shown. The difference between the two methods was expressed by the P value indicated for each analyzed immune cell population. *P* values calculated by Wilcoxon matched-pairs signed rank test.

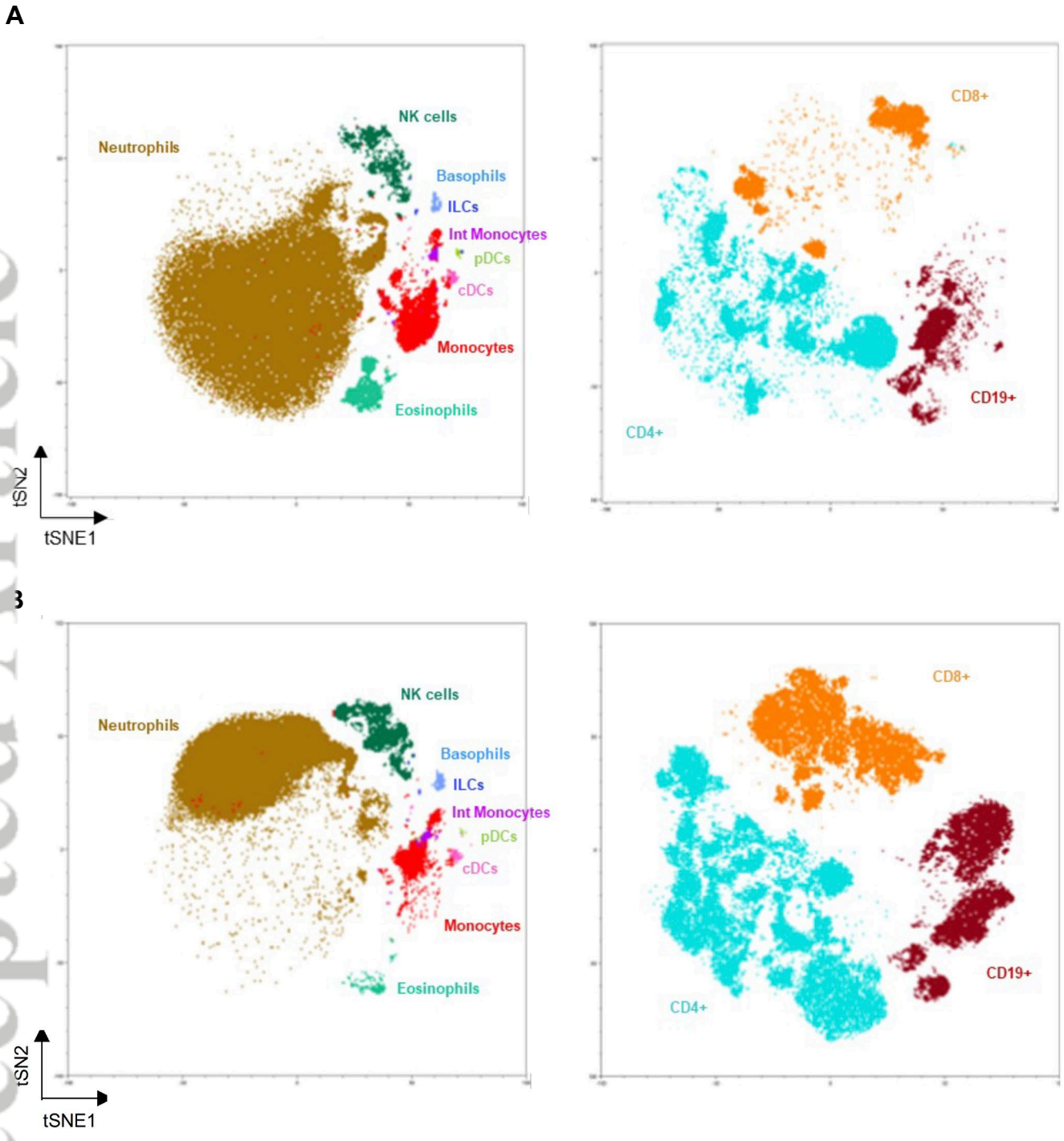

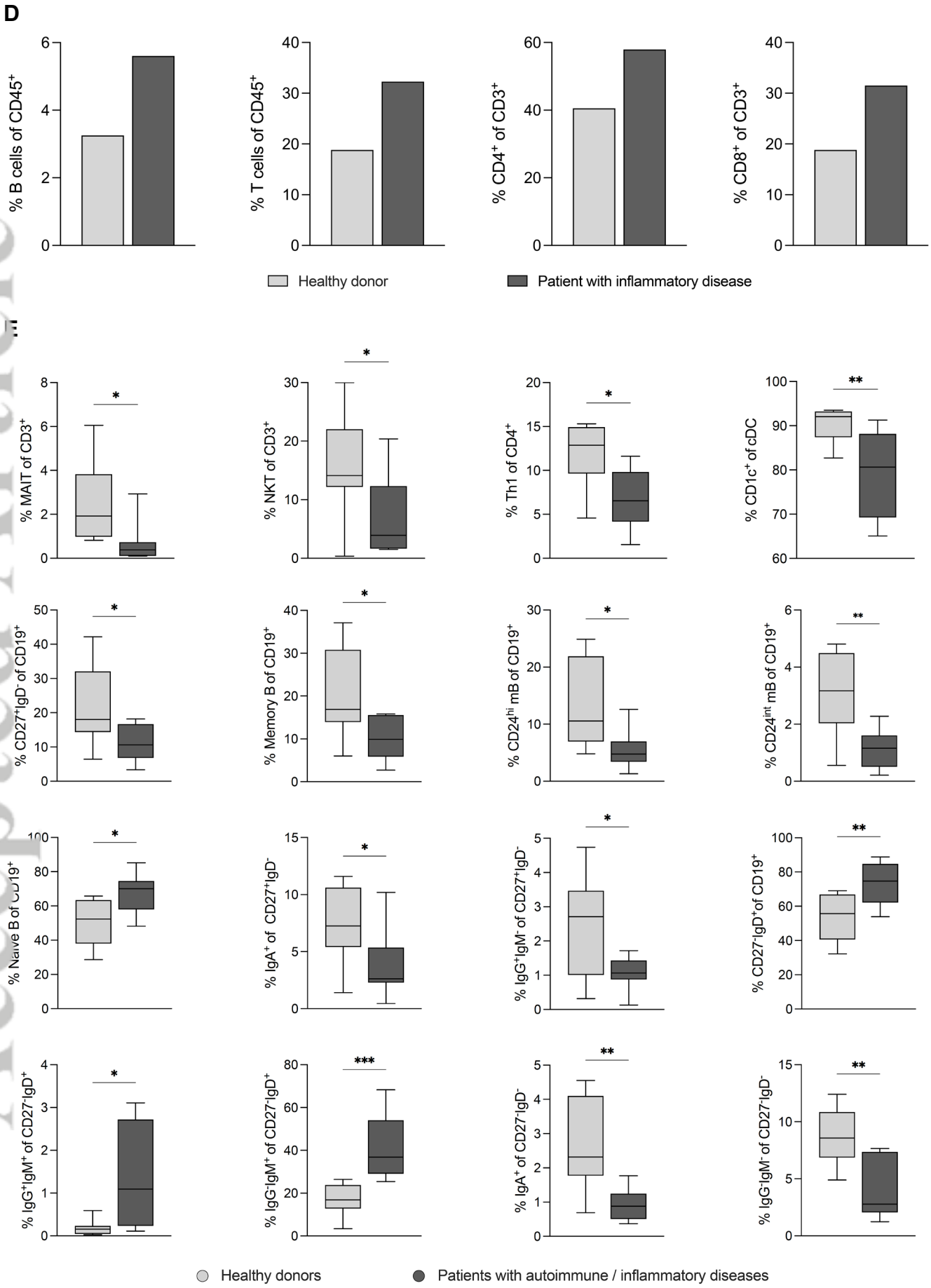

Figure 6. Supervised and unsupervised analysis of healthy and patient data. Fresh blood from 8 patients with autoimmune/inflammatory disease was analyzed and compared with age/sex-matched donors from MI 10-year follow-up study**.** (A, B) An unsupervised analysis was performed by the prototype of Sony software. The input data were single alive dump negative cells. Data from one healthy and one patient subject were concatenated prior to the unsupervised analysis. We used 750 iterations and the perplexity of 30 as parameters for creating the Flt-SNE representations. KNN algorithm was used for clustering. Shown are tSNE projections of clusters annotated based on manual gating. A representative example of a healthy donor (A) and of a patient with an inflammatory disease (B), is shown for innate panel (left) and adaptive panel (right). (C, D) Phenotypes characterized by supervised (FlowJo) analysis of the same subjects and the same immune cell populations as for unsupervised analysis, for innate panel (C) and adaptive panel (D). (E) Supervised analysis of eight patients and matched healthy donors. The unpaired t-test was used for statistical analysis: *, $P<0.05$; **, $P<0.005$; ***, $P<0.0005$.